Int. J. Heat Mass Transfer. Vol. 18, pp. 1267–1276. Pergamon Press 1975. Printed in Great Britain

MOLECULAR GAS RADIATION AND LAMINAR OR TURBULENT HEAT DIFFUSION IN A CYLINDER WITH INTERNAL HEAT GENERATION

A. T. WASSEL,* D. K. EDWARDS† and I. CATTON‡
School of Engineering and Applied Science, University of California, Los Angeles, CA 90024, U.S.A.

(*Received* 15 *January* 1975 *and in revised form* 6 *February* 1975)

Abstract—Simultaneous nongray radiation and thermal diffusion in a thermally and hydrodynamically established laminar or turbulent pipe flow with uniform internal heat generation is treated. The governing integro-differential thermal energy equation is solved using the Galerkin technique for the laminar case and finite difference and numerical iteration techniques for turbulent flow. Solutions are presented for radiative and convective Nusselt number as a function of the radiation to molecular conductance ratio N_{rm}, the optical depth τ_R along the radius at a photon wavenumber spectrally located at the head of an exponential-tailed absorption band, and a turbulent Reynolds number R_t. The radiative Nusselt number is found to increase almost linearly with N_{rm} and linearly with τ_R at small τ_R but approximately logarithmically at large τ_R. The radiative transfer also increases with increasing turbulence R_t, as the turbulence improves the effective wall layer gas transmissivity.

NOMENCLATURE

A^+, van Driest universal constant;
A_a, axial band absorptance;
a_n, Galerkin coefficient;
B_ν, spectral black body radiosity;
B'_ν, derivative of B_ν with respect to r;
B_{nj}, matrix;
c, speed of light;
C_p, specific heat at constant pressure;
C_f, coefficient of friction;
$\mathbf{D}_j$, vector;
E_1, exponential integral function;
G^*, dimensionless radiant flux;
h, Planck's constant;
K, von Karman constant;
k, number of bands;
k_m, molecular conductivity;
k_ν, spectral mass absorption coefficient;
k, Boltzmann constant;
N, number of Galerkin terms;
N_{rm}, radiation to molecular conductance ratio;
Nu_C, convective Nusselt number;
Nu_R, radiative Nusselt number;
Nu_T, total Nusselt number;
P, pressure;
Pr, Prandtl number;
Pr_t, turbulent Prandtl number;
Pr_{eff}, effective Prandtl number;
q_C, convective heat flux;
q_R, radiative heat flux;
$\dot{Q}_V$, volumetric heat source;
r, r', radial coordinate;
R, cylinder radius;
R_t, turbulent Reynolds number;
Re_D, Reynolds number;
T, temperature;
u, local velocity;
V, bulk velocity;
W_i, dimensionless weighting parameter;
x, argument;
y, distance from the wall $(R-r)$;
y_t, transition distance;
z, axial coordinate.

Greek symbols

α_i, integrated band intensity;
α, absorptivity;
α_m, thermal diffusivity;
γ_e, Euler–Mascheroni constant = 0·5772156...;
ε, emissivity;
ε_H, eddy diffusivity for heat;
ε_M, eddy diffusivity for momentum;
θ, dimensionless temperature;
λ, empirical universal constant;
ν_m, molecular kinematic viscosity;
ν, wavenumber, reciprocal wavelength;
π, 3·141592...;
ρ, gas density;
σ, Stefan–Boltzmann constant;
τ_{wb}, wall layer transmissivity;
τ, shear stress;
τ_R, optical depth of the tube radius at maximum absorption;
ω, band wing decay width parameter.

Subscripts

C, convective;
cl, centerline;
H, heat;
i, ith band;
i, ith node point;

* Presently at Science Applications, Inc., El Segundo, CA 90245, U.S.A.
† Professor of Engineering and Applied Science.
‡ Associate Professor of Engineering and Applied Science.

M, momentum;
m, molecular;
R, radiative;
T, total;
t, turbulent, transition;
v, volume average;
w, wall;
ν, spectral.

Superscripts

*, dimensionless quantity;
+, dimensionless turbulent quantity.

INTRODUCTION

IN ENGINEERING practice, it is often necessary to estimate the heat transfer to the walls of a reactor or a combustion chamber or to the melt surface in a furnace. Turbulent diffusion and thermal radiation, which are the two major mechanisms, serve to transfer heat from hot combustion gases to cooler regions. One is interested in knowing how much does a cold gas layer adjacent to a wall reduce the heat transfer to it. Heat transfer also affects the combustion process, because heat release and removal rates fix the combustion gas temperature, which in turn influences the thermodynamic and kinetic parameters. For example, formation of nitric oxide in the gases of fossil-fuel-fired boilers and internal combustion engines is strongly affected by combustion temperature [1, 2]. The quenched layer adjacent to the cooled walls in internal combustion engines contributes to incomplete combustion. Incomplete combustion is wasteful of energy, and the unwanted hydrocarbons and carbon monoxide exhaust products pollute the atmosphere or add to the problem of heat removal from a catalytic after-burner. The thickness of the quenched layer is strongly affected by simultaneous radiation and turbulent transport. In addition to the abovementioned applications, heat transfer by simultaneous radiation and convection appears in almost any engineering system operating at high temperatures, for example an arc or plasma.

Viskanta [3] studied the interaction of conduction, laminar convection, and radiation in a plane layer of a radiating fluid. Other good reviews for the case of pure convection (or laminar Couette flow) and gray radiation can be found in papers by Cess [4] and Viskanta [5]. Einstein [6] considered radiant heat transfer in an absorbing–emitting gray gas flowing within a black-walled cylindrical pipe. Nichols [7] studied the influence of the absorption of radiation on the temperature profile and heat transfer to an absorbing medium flowing turbulently in an annulus. deSoto and Edwards [8] predicted the radiative interchange between a black tube wall and a nonisothermal nongray gas with prescribed temperature. deSoto [9] investigated the coupling of radiation with conduction and convection in a nonisothermal, nongray gas flowing in the entrance region of a black-walled tube in a purely numerical approach. Kesten [10] presented the equations for the spectral radiant heat flux distribution in an absorbing–emitting gas contained in a long cylinder whose internal surface is black.

Landram *et al.* [11] studied heat transfer in turbulent pipe flow with optically thin radiation. Habib and Greif [12] investigated nongray radiative transport in a cylindrical medium. Tiwari and Cess [13] examined heat transfer to laminar flow of nongray gases through a circular tube. These latter two analyses [12, 13] are based upon an approximation suitable only for the optically thick limit [14, 15] and are thus of limited validity for a molecular gas having radiation transfer occurring in optically thin band wings. Edwards and Balakrishnan [16, 17] used a slab band absorptance function to investigate simultaneous radiation, turbulent transport, and internal heat source in plane parallel ducts. They treated both linear and nonlinear cases. Wassel and Edwards [18] formulated the radiative flux in a cylinder in terms of an axial band absorptance function. Closed-form expressions for this latter quantity were obtained for cases when gas properties can be represented by the exponential-winged band model.

It is the purpose of this paper to investigate the interaction of the different modes of energy transfer, hence, to modify the commonly-used well-stirred model [19], where the total heat transfer is computed by adding an isothermal–gas–radiative flux to a convective one. A laminarly or turbulently flowing radiating gas with a constant volume heat source and enclosed by a black-walled cylinder is considered.

MATHEMATICAL FORMULATION

Radiative flux

For black walls the radiative flux can be written as follows [18]:

$$q_R(r^*) = \sum_{i=1}^{k} q_{R,i}(r^*) \tag{1}$$

$$\begin{aligned} q_{R,i}(r^*) = \omega_i \int_{\gamma=0}^{\pi/2} \cos\gamma \Bigg\{ & \int_{r^*}^{1} B'_{\nu_i}(r^{*\prime}) A^*_{a,i}(\\ & \times \tau_{R,i}[(r^{*\prime 2} - r^{*2}\sin^2\gamma)^{\frac{1}{2}} - r^*\cos\gamma])\,\mathrm{d}r^{*\prime} \\ & - \int_{r^*\sin\gamma}^{1} B'_{\nu_i}(r^{*\prime}) A^*_{a,i}(\tau_{R,i} \\ & \times [(r^{*\prime 2} - r^{*2}\sin^2\gamma)^{\frac{1}{2}} + r^*\cos\gamma])\,\mathrm{d}r^{*\prime} \\ & + \int_{r^*\sin\gamma}^{r^*} B'_{\nu_i}(r^{*\prime}) A^*_{a,i}(\tau_{R,i}[r^*\cos\gamma \\ & \qquad - (r^{*\prime 2} - r^{*2}\sin^2\gamma)^{\frac{1}{2}}])\,\mathrm{d}r^{*\prime} \Bigg\}\,\mathrm{d}\gamma \end{aligned} \tag{2}$$

where

$$r^* = r/R\,; \quad r^{*\prime} = r'/R \tag{3}$$

$$B'_{\nu_i}(r^{*\prime}) = \frac{\mathrm{d}}{\mathrm{d}r^{*\prime}}[B_{\nu_i}(r^{*\prime})]\,; \quad B_{\nu_i}(r^{*\prime}) = \frac{2\pi\hbar c^2 \nu^3}{\mathrm{e}^{\hbar c\nu/kT(r^{*\prime})} - 1}. \tag{4}$$

The axial band absorptance function $A^*_{a,i}$ was approximated as follows [18]:

$$A^*_{a,i}(x_i) = \ln(4x_i/\pi) + E_1(4x_i/\pi) + \gamma_e, \quad x_i \leqslant 0{\cdot}38 \tag{5a}$$

$$A^*_{a,i}(x_i) = \ln x_i + E_1(3\pi x_i/8) + \gamma_e + \ln 2 - \tfrac{1}{2}, \quad x_i > 0{\cdot}38 \tag{5b}$$

where

$$x_i = \tau_{R,i}\bar{r}^*; \quad \tau_{R,i} = \frac{\alpha_i}{\omega_i}\rho R$$

$$\bar{r}^* = \eta r^* \cos\gamma + \xi(r^{*2} - r^{*2}\sin^2\gamma)^{\frac{1}{2}}$$

$$E_1(x) = \int_0^1 e^{-x/t}\frac{dt}{t} = \int_1^\infty e^{-xt}\frac{dt}{t}$$

$$\gamma_e = \int_0^1 (1-e^{-t})\frac{dt}{t} - \int_1^\infty e^{-t}\frac{dt}{t} = 0{\cdot}5772156\ldots.$$

The parameters of η and ξ take the values ± 1. Equation (5) holds for gases whose spectral absorption coefficient, k_ν, can be represented by the exponential-winged band model, that is,

$$k_\nu = \sum_{i=1}^{k} k_{\nu_i}; \quad k_{\nu_i} = \frac{\alpha_i}{\omega_i}\exp[-(\nu_i - \nu)/\omega_i], \quad \nu < \nu_i$$

where α_i is the integrated intensity of the ith band, ω_i is the band wing decay width and ν_i is the spectral location of the band head [20].

Governing equation and boundary conditions

The thermal energy equation describing a thermally established, laminar or turbulent, radiating gas with a volume heat source, $\dot{Q}_V$, can be written as follows

$$\frac{\rho C_p}{r}\frac{d}{dr}\left[(\alpha_m + \varepsilon_H)r\frac{dT}{dr}\right] - \frac{1}{r}\frac{d}{dr}(rq_R) + \dot{Q}_V = 0. \quad (6a)$$

For a laminarly flowing gas the turbulent heat diffusivity ε_H is zero, leaving only the molecular coefficient α_m. The above integral-differential equation is subject to the boundary conditions

$$r = 0 : \frac{dT}{dr} = 0; \quad r = R : T = T_w. \quad (6b)$$

The first term of equation (6a) represents the laminar and turbulent diffusion which depends on the molecular properties of the fluid, flow conditions and local temperature gradient. The second term represents the radiative flux which depends on the fluid properties and the overall temperature field and is given by equation (1). The eddy diffusivity for heat, ε_H, is described by a model of turbulence. Assuming a constant $\dot{Q}_V$, integrating equation (6a), making use of the symmetry, and rendering the equation dimensionless yields

$$\varepsilon^*\frac{dT^*}{dr^*} - q_R^* + r^* = 0 \quad (7)$$

where

$$\varepsilon^* = (1 + \varepsilon_H/\alpha_m) = Pr\,Pr_{\text{eff}}^{-1}(1 + \varepsilon_M/\nu_m) \quad (8a)$$

$$Pr_{\text{eff}} = (1 + \varepsilon_M/\nu_m)/[Pr^{-1} + Pr_t^{-1}(\varepsilon_M/\nu_m)]; \quad Pr_t = \varepsilon_M/\varepsilon_H \quad (8b)$$

$$T^* = (T - T_w)/(\dot{Q}_V R^2/2k_m) \quad (8c)$$

$$q_R^*(r^*) = q_R/(\dot{Q}_V R/2) = N_{rm}\sum_{i=1}^{k} \mathscr{W}_i G_i^*(\tau_{R,i}, r^*, dT^*/dr^*) \quad (8d)$$

$$N_{rm} = \sum_{i=1}^{k} \omega_i(dB_{\nu_i}/dT)/(k_m/R) \quad (9)$$

$$\mathscr{W}_i = \omega_i(dB_{\nu_i}/dT)\Big/\sum_{i=1}^{k}\omega_i(dB_{\nu_i}/dT) \quad (10)$$

and

$$G_i^*(\tau_{R,i}, r^*) = \int_{\gamma=0}^{\pi/2}\cos\gamma\left\{\int_{r^*}^{1}\frac{dT^*}{dr^{*\prime}}(r^{*\prime}) \times A_{a,i}^*(\tau_{R,i}[(r^{*\prime 2} - r^{*2}\sin^2\gamma)^{\frac{1}{2}} - r^*\cos\gamma])dr^{*\prime} - \int_{r^*\sin\gamma}^{1}\frac{dT^*}{dr^{*\prime}}(r^{*\prime})A_{a,i}^*(\tau_{R,i} \times [(r^{*\prime 2} - r^{*2}\sin^2\gamma)^{\frac{1}{2}} + r^*\cos\gamma])dr^{*\prime} + \int_{r^*\sin\gamma}^{r^*}\frac{dT^*}{dr^{*\prime}}(r^{*\prime})A_{a,i}^*(\tau_{R,i} \times [r^*\cos\gamma - (r^{*\prime 2} - r^{*2}\sin^2\gamma)^{\frac{1}{2}}])dr^{*\prime}\right\}d\gamma \quad (11)$$

The parameter N_{rm} measures the nongray radiation conductance to molecular conductance. The dimensionless weighting parameter, $\mathscr{W}_i$, can be viewed as a measure of the fraction of the total radiative energy transfer contributed by the ith band of a multi-band gas in the large-path-length limit.

The dimensionless energy equation, equation (7), is subject to the boundary condition

$$r^* = 1 : T^* = 0 \quad (12)$$

and is to be solved by an appropriate method. If only a single band is considered, the summation over the bands disappears, and the weighting parameter $\mathscr{W}_i$ becomes unity.

Eddy diffusivity model

The turbulent form of equation (7) can be solved only if one makes an assumption regarding ε^*. The turbulent Prandtl number, Pr_t, relates ε_H to the eddy diffusivity for momentum, ε_M, which can be described by one of many eddy viscosity models. The model used here is a two-layer model, which involves a near-wall region formulation and another formulation for the outer wake-like region. The inner wall region is described by the van Driest model of turbulence [21] modified by Patankar and Spalding [22]. In this model the local damping is affected by the local shear stress rather than the wall value. In the outer part of the flow the mixing length is taken as uniform and proportional to the cylinder radius.

$$\varepsilon_M = K^2y^2[1 - \exp(-y(\tau/\rho)^{\frac{1}{2}}/\nu_m A^+)]^2\left|\frac{du}{dy}\right| \quad \text{for} \quad 0 < y < y_t \quad (13a)$$

$$\varepsilon_M = \lambda^2 R^2\left|\frac{du}{dy}\right| \quad \text{for} \quad y_t < y < R \quad (13b)$$

where y is the distance measured from the wall ($y = R - r$) and y_t is a transition distance at which the above expressions match. The velocity gradient, du/dy, and the local shear stress, τ, are determined by solving the momentum equation for a hydrodynamically established flow,

$$0 = -\frac{1}{\rho}\frac{dP}{dz} + \frac{1}{r}\frac{d}{dr}\left[(\nu_m + \varepsilon_M)r\frac{du}{dr}\right] \quad (14)$$

where dP/dz is the pressure gradient along the cylinder axis. Equation (14) is subject to the boundary conditions

$$r = 0 : \frac{du}{dr} = 0; \quad r = R : u = 0 \tag{15}$$

Integrating equation (14) and making use of the symmetry yields

$$\frac{1}{2\rho}\frac{dP}{dz} r = (\nu_m + \varepsilon_M)\frac{du}{dr} = (\tau_w/\rho)(-r/R) \tag{16}$$

where

$$(\tau/\rho) = -(\nu_m + \varepsilon_M)\frac{du}{dr}.$$

The momentum equation, equation (16), the eddy diffusivity expression, equation (13), and the no-slip boundary condition at the wall, equation (15), can be rewritten as follows:

$$(1 + \varepsilon_M/\nu_m)\frac{du^+}{dr^+} = -r^+/R_t \tag{17a}$$

$$(\varepsilon_M/\nu_m) = -K^2(R_t - r^+)^2 \times \{1 - \exp[-(R_t - r^+)(r^+/R_t)^{\frac{1}{2}}/A^+]\}^2 \frac{du^+}{dr^+} \quad \text{for} \quad r_t^+ \leqslant r^+ \leqslant R_t \tag{17b}$$

$$(\varepsilon_M/\nu_m) = -(\lambda R_t)^2 \frac{du^+}{dr^+} \quad \text{for} \quad 0 \leqslant r^+ \leqslant r_t^+ \tag{17c}$$

$$r^+ = R_t : u^+ = 0 \tag{17d}$$

where

$$u^+ = u/(\tau_w/\rho)^{\frac{1}{2}}; \quad r^+ = r(\tau_w/\rho)^{\frac{1}{2}}/\nu_m = R_t - y^+$$
$$R_t = R(\tau_w/\rho)^{\frac{1}{2}}/\nu_m$$

and r_t^+ is a transition radius at which the eddy viscosity given by equations (17b) and (17c) have the same value. The quantity $K = 0{\cdot}4$ is von Karman's constant, $A^+ = 30$ is a universal constant, and $\lambda = 0{\cdot}075$. The values of the above empirical constants were re-evaluated by numerical experiments to match available data of skin friction and dimensionless velocity profile [21–25]. The turbulent Reynolds number, R_t, is related to the Reynolds number, based on the cylinder diameter, through the relation

$$R_t = (C_f/8)^{\frac{1}{2}} Re_D \tag{18a}$$

$$Re_D = \frac{V2R}{\nu_m} = \frac{4}{R_t}\int_0^{R_t} u^+(r^+) r^+ \, dr^+ \tag{18b}$$

$$C_f = (\tau_w/\rho)/\tfrac{1}{2}V^2 = 8(R_t/Re_D)^2. \tag{18c}$$

The quantity r^+ is related to r^* through the relation

$$r^+ = R_t r^*. \tag{18d}$$

Note that R_t is r^+ at $r = R$, or what one might denote as R^+.

The system of equations, (17a)–(17d), are solved first by a numerical iteration procedure to yield the $\varepsilon_M(r^*)/\nu_m$ distribution, hence the $\varepsilon^*(r^*)$ profile with parameter R_t or Re_D.

Nusselt numbers, average temperature, and effective transmissivity

The average temperature considered here is the volume average temperature defined as

$$(T_v - T_w) = \int_0^R (T - T_w) 2\pi r \, dr \Big/ \int_0^R 2\pi r \, dr. \tag{19}$$

From the definition of the dimensionless temperature T^*, equation (8c), equation (19) can be rewritten as

$$T_v^* = 2\int_0^1 T^*(r^*) r^* \, dr^*. \tag{20}$$

The convective Nusselt number is defined as

$$Nu_C = \frac{q_{C,w} 2R}{k_m(T_v - T_w)} = -2\left.\frac{dT^*}{dr^*}\right|_{r^*=1} \Big/ T_v^*. \tag{21}$$

The radiative Nusselt number can be written as

$$Nu_R = \frac{q_{R,w} 2R}{k_m(T_v - T_w)} = 2q_R^*(r^* = 1)/T_v^*. \tag{22}$$

The total Nusselt number is the sum of Nu_C and Nu_R,

$$Nu_T = Nu_C + Nu_R. \tag{23}$$

The peak to average temperature ratio is given by

$$\theta = \frac{T_{cl} - T_w}{T_v - T_w} = T_{cl}^*/T_v^*. \tag{24}$$

The wall layer effective transmissivity, τ_{wl}, is also of interest and is defined as follows:

$$\tau_{wl} = \frac{q_{R,w}}{\varepsilon_g \sigma T_v^4 - \alpha_g \sigma T_w^4} = \frac{q_{R,w}}{\sum_{i=1}^{k} [\bar{A}_i B_{\nu_i}(T_v) - \bar{A}_i B_{\nu_i}(T_w)]} \tag{25}$$

where $\bar{A}_i = \omega_i \bar{A}_i^*$ is the mean band absorptance and is given by [18]

$$\bar{A}_i = \omega_i \int_{\gamma=0}^{\pi/2} A_{a,i}^*(2\tau_{R,i}\cos\gamma)\cos\gamma \, d\gamma \tag{26}$$

Linearizing equation (25) and introducing the radiative Nusselt number, Nu_R, allows the wall layer transmissivity to be written as follows, provided a single band (or a number of identical bands) is considered.

$$\tau_{wl} = \tfrac{1}{2}[Nu_R/\bar{A}^*][(k_m/R)(\omega \, dB_\nu/dT)] = \tfrac{1}{2}Nu_R/[\bar{A}^* N_{rm}] \tag{27}$$

Values of $\bar{A}^*$ as function of τ_R can be found in reference [18].

METHODS OF SOLUTION

The laminar case

The solution to equation (7) with $\varepsilon^* = 1$ is obtained by the Galerkin technique. The temperature $T^*(r^*)$ is expanded in a series of the form

$$T^*(r^*) \doteq T_0^*(r^*) + \sum_{n=1}^{N} a_n T_n^*(r^*). \tag{28}$$

One substitutes the above into equation (7) to obtain

$$\sum_{n=1}^{N} a_n \left\{\frac{dT_n^*}{dr^*} - N_{rm} G_n^*\left(\tau_R, r^*, \frac{dT_n^*}{dr^*}\right)\right\} = -\left\{r^* + \frac{dT_0^*}{dr^*} - N_{rm} G_0^*\left(\tau_R, r^*, \frac{dT_0^*}{dr^*}\right)\right\}$$

where G_0^* and G_n^* are the parts of the function G^* that depend on dT_0^*/dr^* and dT_n^*/dr^* respectively. If the above equation is multiplied by $T_j^*(r^*)$ and volume-integrated, there results

$$\sum_{n=1}^{N} a_n B_{nj} = \mathbf{D}_j \quad j = 1,2,\ldots N \tag{29}$$

where

$$B_{nj} = \int_0^1 \left\{\frac{dT_n^*}{dr^*} - N_{rm} G_n^*\left(\tau_R, r^*, \frac{dT_n^*}{dr^*}\right)\right\} T_j^* r^* dr^*$$

$$\mathbf{D}_j = -\int_0^1 \left\{r^* + \frac{dT_0^*}{dr^*} - N_{rm} G_0^*\left(\tau_R, r^*, \frac{dT_0^*}{dr^*}\right)\right\} T_j^* r^* dr^*.$$

The coefficients a_n are found by inverting the matrix B_{nj}. The number of terms in the series expansion, equation (28), is increased until a convergence of the solution appears. Seven terms were found adequate. Numerical integrations involved in the Galerkin scheme were performed by the Simpson rule, where the domain of integration is divided into N equal steps. The trial functions that are found to be appropriate are

$$T_0^*(r^*) = 1 - r^{*2}; \quad T_n^*(r^*) = 1 - r^{*2n}.$$

It is to be noted that the parabolic profile considered is the solution to the laminar energy equation for the case of no radiation.

The turbulent case

To avoid needing a large number of terms to describe properly the behavior of a turbulent sublayer, the solution to the turbulent energy equation is obtained adopting a numerical iterative scheme. The interval (0, 1) is divided into N unequal steps where many node points are stacked near the wall in a logarithmic fashion appropriate to turbulent flows. By locating the node points at equal steps in the z^*-plane, the corresponding locations in the r^*-plane can be found,

$$z^* = \ln[1 + KR_t(1 - r^*)]; \quad r_i^* = 1 - \frac{1}{KR_t}(e^{z^i} - 1),$$

where i denotes the ith node point. Fifty-one node points were used.

Having established the node point distribution, the momentum equation is solved first for a given value of the turbulent Reynolds number, R_t, hence establishing the $\varepsilon^*(r^*)$ profile. The energy equation is then solved iteratively. Iteration is repeated until a maximum difference between two successive iterates is less than some prescribed value. After one establishes the dT^*/dr^* profile, the temperature profile can be extracted by making use of the boundary condition at the wall, i.e. $T_{N+1}^*(r^* = 1) = 0$ and integrating.

RESULTS AND DISCUSSION

Results for turbulent flow

Table 1 gives computed radiative, convective and total Nusselt numbers, centerline temperature to volume average temperature ratios and the wall layer transmissivity for $R_t = 200$, 500, 1000 and 2000 respectively and $Pr_t = 0{\cdot}9$. Tabulations are for values of N_{rm} from 0 to 100 and for τ_R from 1 to 200.

It can be seen from the table that at low values of N_{rm} turbulent transfer dominates, while at large values of N_{rm} radiation contributes markedly to the total heat transfer. The radiative flux measured by Nu_R increases in approximately a linear fashion with N_{rm}. It can also be seen that radiative fluxes increase with τ_R first at a high rate then at a lower rate at high values of τ_R for given values of R_t, which characterizes the turbulence, and N_{rm}, which characterizes the nongray gas radiation.

Increasing the turbulent Reynolds number R_t increases markedly the convective transfer to the wall. For example, increasing R_t from 500 ($Re_D = 16\,901$) to 2000 ($Re_D = 80\,650$) increases the convective Nusselt number from 49·9 to 161·2. As a result of the convective phenomena a thin cold layer adjacent to the wall is formed. This thin boundary layer partially shields the wall from the full hot core radiation, and the thicker the layer the less radiation is transferred to the wall. Increasing R_t thins the layer. The resulting effect on radiative transfer can be seen when comparing the results of Nu_R at different values of R_t.

To see the effect of coupling of radiation and turbulence on convective transport consider the values of Nu_C at constant τ_R. Increasing N_{rm} does increase convective transfer significantly at low values of R_t where higher temperature gradients as well as lower volume average temperatures are obtainable. At high values of R_t, convective Nusselt number decreases very slightly due to radiation lowering temperature gradients at the wall. At high values of R_t, the convective Nusselt number can be estimated by the convective empirical correlations without the need to account for the interaction between radiation and turbulence. From Table 1 for $R_t = 2000$ and $\tau_R = 50$ it can be seen that the value of convective Nusselt number at $N_{rm} = 100$ is only 7 per cent below its value of $N_{rm} = 0$.

Radiative transfer decreases the difference between the centerline and wall temperatures for the same amount of heat released, because the radiative mechanism increases the heat transfer to the wall. Figure 1 shows plots of temperature profiles normalized by the volume average temperature. The temperature profiles intersect because of the normalization of the same (unit) volume average temperature. The centerline (peak) to volume average temperature ratio increases with increase in N_{rm}. The temperature in the outer region decreases as N_{rm} increases (except in the region very close to the wall where a slight increase in the temperature gradient may occur, depending upon the value of R_t), and a higher temperature is obtained in the central region. The opposite, however, is found in the optically thin limit or at low values of τ_R with low turbulence ($R_t = 200$). Table 1 and Fig. 1 show that the centerline-to-volume-average-temperature ratio decreases with increase in N_{rm}, because the temperature in the region near to the wall increases with increase in N_{rm}, thus requiring a lower centerline temperature in order to have the same normalized volume average temperature. The decrease in the peak-to-average-temperature ratio becomes less with increase in R_t.

Table 1. Turbulent flow results

N_{rm}		$\tau_R = 1$	$\tau_R = 10$	$\tau_R = 50$	$\tau_R = 100$	$\tau_R = 200$
		$R_t = 200 (Re_D = 5693)$				
0·0	Nu_C	24·468	24·468	24·468	24·468	24·468
	Nu_R	0·0	0·0	0·0	0·0	0·0
	Nu_T	24·468	24·468	24·468	24·468	24·468
	T_{cl}^*/T_v^*	1·439	1·439	1·439	1·439	1·439
0·1	Nu_C	24·495	24·530	24·538	24·541	24·544
	Nu_R	0·244	0·566	0·662	0·678	0·686
	Nu_T	24·739	25·096	25·200	25·219	25·230
	T_{cl}^*/T_v^*	1·438	1·439	1·440	1·440	1·440
	τ_{wl}	0·9710	0·8179	0·6530	0·5884	0·5314
1·0	Nu_C	24·736	25·081	25·164	25·197	25·230
	Nu_R	2·441	5·663	6·614	6·768	6·849
	Nu_T	27·177	30·744	31·778	31·965	32·079
	T_{cl}^*/T_v^*	1·432	1·437	1·445	1·446	1·445
	τ_{wl}	0·9714	0·8183	0·6524	0·5873	0·5305
10·0	Nu_C	26·988	30·155	31·140	31·446	31·721
	Nu_R	24·455	56·877	65·938	67·417	68·245
	Nu_T	51·443	87·032	97·078	98·863	99·966
	T_{cl}^*/T_v^*	1·379	1·426	1·465	1·468	1·466
	τ_{wl}	0·9732	0·8219	0·6504	0·5850	0·5286
100·0	Nu_C	42·702	62·555	68·293	69·491	70·395
	Nu_R	246·361	579·017	670·651	687·002	697·284
	Nu_T	289·064	641·572	738·944	756·493	767·679
	T_{cl}^*/T_v^*	1·222	1·396	1·464	1·469	1·468
	τ_{wl}	0·9804	0·8367	0·6616	0·5962	0·5401
		$R_t = 500 (Re_D = 16\,901)$				
0·0	Nu_C	49·873	49·873	49·873	49·873	49·873
	Nu_R	0·0	0·0	0·0	0·0	0·0
	Nu_T	49·873	49·873	49·873	49·873	49·873
	T_{cl}^*/T_v^*	1·354	1·354	1·354	1·354	1·354
0·1	Nu_C	49·889	49·896	49·885	49·884	49·884
	Nu_R	0·246	0·596	0·732	0·760	0·775
	Nu_T	50·135	50·492	50·617	50·644	50·659
	T_{cl}^*/T_v^*	1·354	1·354	1·355	1·355	1·355
	τ_{wl}	0·9790	0·8612	0·7221	0·6595	0·6003
1·0	Nu_C	50·025	50·095	49·999	49·987	49·995
	Nu_R	2·459	5·955	7·300	7·577	7·725
	Nu_T	52·484	56·050	57·299	57·564	57·720
	T_{cl}^*/T_v^*	1·352	1·356	1·361	1·362	1·362
	τ_{wl}	0·9786	0·8605	0·7201	0·6575	0·5984
10·0	Nu_C	51·345	52·196	51·772	51·809	51·963
	Nu_R	24·598	59·319	71·685	74·099	75·400
	Nu_T	75·943	111·515	123·457	125·908	127·363
	T_{cl}^*/T_v^*	1·332	1·368	1·400	1·405	1·405
	τ_{wl}	0·9789	0·8572	0·7071	0·6430	0·5840
100·0	Nu_C	61·969	73·246	77·048	78·428	79·683
	Nu_R	246·882	589·182	691·350	709·971	721·443
	Nu_T	308·851	662·428	768·398	788·399	801·126
	T_{cl}^*/T_v^*	1·232	1·381	1·449	1·454	1·453
	τ_{wl}	0·9825	0·8514	0·6820	0·6161	0·5588

One may compare the predicted convective Nusselt number based on volume average temperature with that of turbulent pipe flow for a transparent gas of $Pr = 0{\cdot}7$. At low values of R_t the computed Nu_C is within 20 per cent of the modified Dittus–Boelter formula $Nu_C = 0{\cdot}023 Re_D^{0{\cdot}8} Pr^{0{\cdot}33}$. At higher values of R_t the predicted Nu_C is within 7 per cent of the empirical formula. Although the results are for a uniform heat source, they are in fair agreement with pipe flow predictions.

Table 1 shows that the wall layer effective transmissivity, τ_{wl}, can assume a value as low as 0·53 at low R_t and high τ_R. Transmissivity does increase with increasing the turbulent Reynolds number R_t, due to less blockage of radiation caused by the cold gas layer adjacent to the wall. Transmissivity decreases with

Table 1 (continued)

N_{rm}		$\tau_R = 1$	$\tau_R = 10$	$\tau_R = 50$	$\tau_R = 100$	$\tau_R = 200$
		$R_t = 1000 (Re_D = 37\,185)$				
0·0	Nu_C	88·961	88·961	88·961	88·961	88·961
	Nu_R	0·0	0·0	0·0	0·0	0·0
	Nu_T	88·961	88·961	88·961	88·961	88·961
	T_{cl}^*/T_v^*	1·314	1·314	1·314	1·314	1·314
0·1	Nu_C	88·971	88·965	88·942	88·935	88·932
	Nu_R	0·247	0·611	0·775	0·816	0·841
	Nu_T	89·218	89·576	89·717	89·751	89·773
	T_{cl}^*/T_v^*	1·313	1·314	1·314	1·314	1·314
	τ_{wl}	0·9830	0·8829	0·7645	0·7081	0·6514
1·0	Nu_C	89·063	89·006	88·780	88·714	88·680
	Nu_R	2·466	6·107	7·735	8·136	8·385
	Nu_T	91·529	95·113	96·515	96·850	97·063
	T_{cl}^*/T_v^*	1·312	1·315	1·319	1·319	1·320
	τ_{wl}	0·9814	0·8825	0·7630	0·7060	0·6495
10·0	Nu_C	89·967	89·546	87·777	87·319	87·132
	Nu_R	24·664	60·851	76·110	79·665	81·816
	Nu_T	114·631	150·397	163·887	166·984	168·948
	T_{cl}^*/T_v^*	1·303	1·329	1·354	1·359	1·361
	τ_{wl}	0·9815	0·8793	0·7508	0·6913	0·6337
100·0	Nu_C	97·763	99·939	97·459	97·660	98·428
	Nu_R	247·174	599·724	717·902	740·806	754·458
	Nu_T	344·937	699·663	815·361	838·466	852·886
	T_{cl}^*/T_v^*	1·242	1·365	1·435	1·443	1·444
	τ_{wl}	0·9837	0·8666	0·7082	0·6429	0·5844
		$R_t = 2000 (Re_D = 80\,650)$				
0·0	Nu_C	161·181	161·181	161·181	161·181	161·181
	Nu_R	0·0	0·0	0·0	0·0	0·0
	Nu_T	161·181	161·181	161·181	161·181	161·181
	T_{cl}^*/T_v^*	1·282	1·282	1·282	1·282	1·282
0·1	Nu_C	161·188	161·175	161·142	161·129	161·121
	Nu_R	0·247	0·623	0·809	0·863	0·900
	Nu_T	161·435	161·798	161·951	161·992	162·021
	T_{cl}^*/T_v^*	1·282	1·282	1·282	1·282	1·282
	τ_{wl}	0·9830	0·9003	0·7980	0·7489	0·6971
1·0	Nu_C	161·253	161·118	160·791	160·670	160·585
	Nu_R	2·473	6·223	8·083	8·613	8·980
	Nu_T	163·726	167·341	168·874	169·282	169·565
	T_{cl}^*/T_v^*	1·281	1·283	1·285	1·285	1·286
	τ_{wl}	0·9842	0·8993	0·7973	0·7474	0·6956
10·0	Nu_C	161·893	160·649	157·729	156·692	156·002
	Nu_R	24·731	62·056	79·903	84·795	88·114
	Nu_T	186·625	222·705	237·632	241·487	244·116
	T_{cl}^*/T_v^*	1·277	1·293	1·310	1·313	1·316
	τ_{wl}	0·9842	0·8967	0·7882	0·7358	0·6825
100·0	Nu_C	167·721	161·380	148·744	145·598	144·265
	Nu_R	247·486	611·010	752·527	784·364	804·291
	Nu_T	415·207	772·390	901·271	929·962	948·556
	T_{cl}^*/T_v^*	1·244	1·339	1·403	1·413	1·417
	τ_{wl}	0·9849	0·8829	0·7423	0·6807	0·6230

increasing optical depth τ_R. The low values of transmissivity show that the cold gas layer absorption can exert a significant influence upon the radiant heat transfer to a reactor wall and hence upon the reactor gas temperature.

Edwards and Balakrishnan [16] investigated combined turbulent diffusion and radiation with an internal heat source in a plane parallel duct. They too found that radiation contribution grows nearly linearly with N_{rm}, and at high values of N_{rm} radiation dominates the total transfer. Increasing R_t increases markedly the convective transport at the wall and significantly raises the radiative transport. They also showed that the peak to volume average temperature ratio increases with increase in N_{rm}. In addition to this qualitative agreement, excellent quantitative agreement exists between

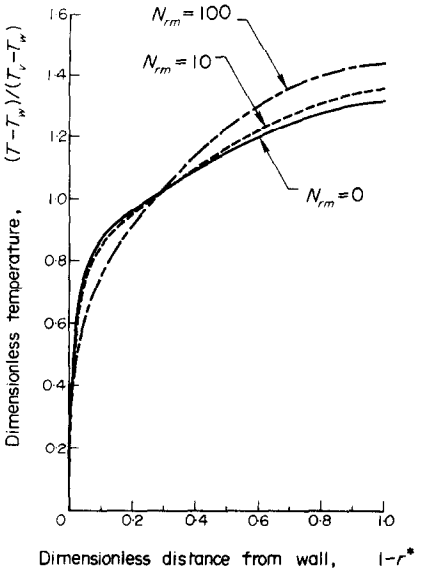

FIG. 1. Temperature profiles for turbulent flow ($R_t = 1000$, $\tau_R = 50$).

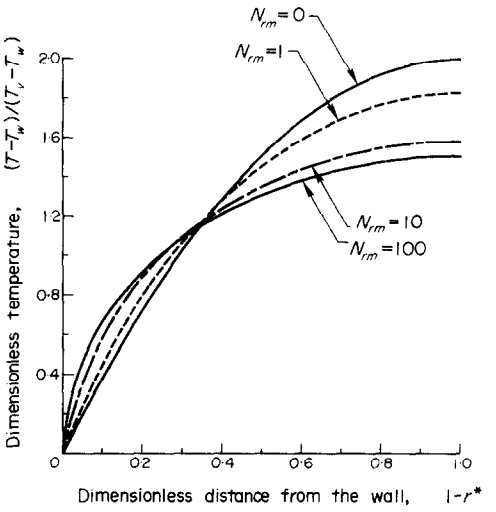

FIG. 2. Temperature profiles for laminar flow ($\tau_R = 50$).

Table 2. Laminar flow results

N_{rm}		$\tau_R = 0{\cdot}1$	$\tau_R = 1$	$\tau_R = 10$	$\tau_R = 50$	$\tau_R = 100$	$\tau_R = 200$
0·0	Nu_C	8·0	8·0	8·0	8·0	8·0	8·0
	Nu_R	0·0	0·0	0·0	0·0	0·0	0·0
	Nu_T	8·0	8·0	8·0	8·0	8·0	8·0
	T_{cl}^*/T_v^*	2·0	2·0	2·0	2·0	2·0	2·0
0·1	Nu_C	8·013	8·099	8·266	8·296	8·297	8·296
	Nu_R	0·038	0·237	0·485	0·533	0·544	0·552
	Nu_T	8·051	8·336	8·751	8·829	8·840	8·848
	T_{cl}^*/T_v^*	1·998	1·988	1·974	1·974	1·974	1·974
	τ_{wl}	1·00	0·9432	0·7008	0·5258	0·4721	0·4276
1·0	Nu_C	8·129	8·937	10·308	10·500	10·481	10·459
	Nu_R	0·378	2·380	4·990	5·565	5·700	5·797
	Nu_T	8·507	11·317	15·295	16·065	16·181	16·256
	T_{cl}^*/T_v^*	1·984	1·895	1·819	1·824	1·826	1·826
	τ_{wl}	0·9963	0·9472	0·7211	0·5490	0·4946	0·4490
10·0	Nu_C	9·206	14·666	20·827	19·920	19·255	18·793
	Nu_R	3·779	24·122	54·246	63·607	65·664	67·027
	Nu_T	12·986	38·788	75·073	83·527	84·920	85·822
	T_{cl}^*/T_v^*	1·861	1·511	1·532	1·582	1·591	1·596
	τ_{wl}	0·9960	0·9600	0·7839	0·6274	0·5698	0·5192
100·0	Nu_C	16·181	36·542	39·443	29·264	26·998	25·639
	Nu_R	37·844	247·070	602·874	710·959	729·428	741·134
	Nu_T	54·024	283·612	642·316	740·223	756·426	766·773
	T_{cl}^*/T_v^*	1·403	1·222	1·419	1·504	1·519	1·527
	τ_{wl}	0·9975	0·9832	0·8712	0·7013	0·6330	0·5741

the present predictions and those of [16] when one compares on the basis of equal optical depths for the geometric mean beam length and equal Reynolds numbers based upon the hydraulic diameter. The optical depth for geometric mean beam length τ_L is related to τ_R in this work by $\tau_R = \frac{1}{2}\tau_L$, and τ_L is related to τ_H for the channel half width in the previous paper [16] by $\tau_H = \frac{1}{4}\tau_L$.

Edwards and Balakrishnan [17] showed that at low values of the optical depth at band head and low turbulence, the centerline to volume average temperature ratio decreases with increasing N_{rm}. The same behavior was noticed by Landram *et al.* [11].

Results for laminar flow

Similar to the turbulent case, radiative transfer dominates the total transfer when the radiation conductance to molecular conductance ratio, N_{rm}, becomes large. Table 2 shows that radiative Nusselt number grows nearly linearly with N_{rm} at small values of τ_R and deviates from the linear increase at high τ_R as well as high N_{rm}. Increasing radiation, measured by N_{rm},

increases markedly the convective transfer at the wall from a value of 8 to a value as high as 5 times that when N_{rm} is increased from 0 to 100. This behavior is similar to the low turbulent case, but more marked, and is opposite to the highly turbulent case.

Radiation decreases the volume average temperature by decreasing the difference between the centerline and wall temperature for a given amount of heat release $\dot{Q}_V$. Therefore higher values of N_{rm} lead to higher convective Nusselt numbers. Figure 2 shows that higher normalized temperature gradients at the wall are obtained with higher N_{rm}. The outer region (near to the wall) becomes hotter with increase in N_{rm} and the central region becomes colder in order to maintain the same volume average temperature. The peak to volume average temperature ratio decreases with increasing N_{rm} for small as well as large values of τ_R. Recall that for the turbulent case the centerline-to-average-temperature ratio decreases with increase in N_{rm} only at low values of R_t and in the thin limit of radiation. For the laminar and low turbulence cases the normalized temperature gradient at the wall increases appreciably with increasing N_{rm}, thus leading to the above observation. It is to be noted that the curve marked $N_{rm} = 0$ in Fig. 2 represents the exact solution to the energy equation for a laminar transparent medium and is given by $T^* = \frac{1}{2}(1-r^{*2})$. The centerline to volume average temperature ratio in this case is 2·0.

The effective layer transmissivity, τ_{wl}, varies between 1·0 and 0·43, and decreases with increasing the optical depth, τ_R, similar to the turbulent case.

REFERENCES

1. B. P. Breen, A. W. Bell, N. Bayard de Volo, A. F. Bagwell and K. Rosenthal, Combustion control for elimination of nitric oxide emissions from fossil-fuel power plants, *Thirteenth Symposium (International) on Combustion*, pp. 391–401. The Combustion Institute, (1970).
2. E. S. Starkman, Theory, experiment, and rationale in the generation of pollutants by combustion, *12th Symposium (International) on Combustion*, pp. 593–601. The Combustion Institute (1968).
3. R. Viskanta, Interaction of heat transfer by conduction, convection, and radiation in radiating fluids, *J. Heat Transfer* **85C**, 318–328 (1963).
4. R. D. Cess, The interaction of thermal radiation with conduction and convection heat transfer, *Advances in Heat Transfer* (edited by T. F. Irvine, Jr., and J. P. Hartnett), Vol. 1, pp. 1–49. Academic Press, New York (1964).
5. R. Viskanta, Radiation transfer and interaction of convection with radiation heat transfer, *Advances in Heat Transfer*, Vol. 3, pp. 176–248. Academic Press, New York (1966).
6. T. H. Einstein, Radiant heat transfer in absorbing gases enclosed in a circular pipe with conduction, gas flow and internal heat generation, NASA TR R-156 (1963).
7. L. D. Nichols, Temperature profile in the entrance region of an annular passage considering the effects of turbulent convection and radiation, *Int. J. Heat Mass Transfer* **8**, 589–607 (1965).
8. S. deSoto and D. K. Edwards, Radiative emission and absorption in nonisothermal nongray gases in tubes, *Proceedings 1965 Heat Transfer and Fluid Mechanics Institute*, pp. 358–372. Stanford University Press, Stanford (1965).
9. S. deSoto, Coupled radiation, conduction and convection in entrance region flow, *Int. J. Heat Mass Transfer* **11**, 39–53 (1968).
10. A. S. Kesten, Radiant heat flux distribution in a cylindrically symmetric nonisothermal gas with temperature dependent absorption coefficient, *Jl Quantve Spectrosc. & Radiat. Transf.* **8**, 419–434 (1968).
11. C. S. Landram, R. Greif and I. S. Habib, Heat transfer in turbulent pipe flow with optically thin radiation, *J. Heat Transfer* **91C**, 330–336 (1969).
12. I. S. Habib and R. Greif, Nongray radiative transport in a cylindrical medium, *J. Heat Transfer* **92C**, 28–32 (1970).
13. S. N. Tiwari and R. D. Cess, Heat transfer to laminar flow of nongray gases through a circular tube, *Appl. Scient. Res.* **25**, 155–169 (1971).
14. D. K. Edwards and A. T. Wassel, The radial radiative heat flux in a cylinder, *J. Heat Transfer* **95C**, 276–277 (1973).
15. Z. Chiba and R. Greif, Discussion of nongray radiative transport in a cylindrical medium, *J. Heat Transfer* **95C**, 142 (1973).
16. D. K. Edwards and A. Balakrishnan, Nongray radiative transfer in a turbulent gas layer, *Int. J. Heat Mass Transfer* **16**, 1003–1015 (1973).
17. D. K. Edwards and A. Balakrishnan, Self-absorption of radiation in turbulent molecular gases, *Combustion and Flame* **20**, 401–417 (1973).
18. A. T. Wassel and D. K. Edwards, Molecular gas band radiation in cylinders, *J. Heat Transfer* **96C**, 21–26 (1974).
19. J. M. Beer and C. R. Howarth, Radiation from flames in furnaces, *Twelfth Symposium (International) on Combustion*, pp. 1205–1217. The Combustion Institute, (1968).
20. D. K. Edwards and A. Balakrishnan, Thermal radiation by combustion gases, *Int. J. Heat Mass Transfer* **16**, 25–40 (1973).
21. E. R. van Driest, On turbulent flow near a wall, *J. Aeronaut. Sci.* **23**, 1007–1011 (1956).
22. S. V. Patankar and D. B. Spalding, *Heat and Mass Transfer in Boundary Layers*. Morgan-Grampian, London (1967).
23. J. Blom, An experimental determination of the turbulent Prandtl number in a developing temperature boundary layer, Presented at the Fourth International Heat Transfer Conference, Paris, Versailles (1970).
24. W. M. Kays, *Convective Heat and Mass Transfer*. McGraw-Hill, New York (1966).
25. R. G. Deissler, Analytical and experimental investigation of adiabatic turbulent flow in smooth tubes, NACA TN 2138 (1950).

RAYONNEMENT MOLECULAIRE DES GAZ ET DIFFUSION THERMIQUE LAMINAIRE OU TURBULENTE DANS UN CYLINDRE AVEC GENERATION INTERNE DE CHALEUR

Résumé—L'article traite du rayonnement non gris et de la diffusion thermique simultanés dans l'écoulement en conduite thermiquement et hydrodynamiquement établi laminaire ou turbulent avec génération interne uniforme de chaleur. L'équation fondamentale intégro-différentielle de l'énergie thermique est résolue à l'aide de la méthode de Galerkin dans le cas laminaire et à l'aide de méthode numériques de

différences finies et d'itération dans le cas turbulent. On présente des solutions donnant le nombre de Nusselt de rayonnement et de convection en fonction du rapport des conductances de rayonnement et de conduction N_{rm}, de la profondeur optique τ_R le long du rayon pour un nombre d'onde de photon localisé dans le spectre au début d'une bande d'absorption à décroissance exponentielle, et d'un nombre de Reynolds de turbulence R_t. Il est trouvé que le nombre de Nusselt de rayonnement augmente presque linéairement avec N_{rm} et linéairement avec τ_R aux faibles valeurs de τ_R, mais de façon à peu près logarithmique aux grandes valeurs de τ_R. Le transfert par rayonnement augmente aussi avec le niveau de turbulence R_t, puisque la turbulence améliore le coefficient de transfert efficace de la couche gazeuse pariétale.

MOLEKULARE GASSTRAHLUNG UND LAMINARE ODER TURBULENTE WÄRMEDIFFUSION IN EINEM ZYLINDER MIT INNERER WÄRMEQUELLE

Zusammenfassung—Es wird gleichzeitige nicht graue Strahlung und thermische Diffusion in einer thermisch und hydrodynamisch ausgebildeten laminaren oder turbulenten Rohrströmung mit gleichförmiger innerer Wärmeerzeugung behandelt. Die maßgebliche thermische Integro-Differential-Energiegleichung wird gelöst, wobei für den laminaren Fall die Galerkin-Technik und für den turbulenten Fall die finite Differenzen- und numerische Iterationstechnik verwendet wird. Es werden Lösungen mitgeteilt, bei denen die Strahlungs- und die konvektive Nusselt–Zahl eine Funktion ist; 1. des Verhältnisses N_{rm} von Strahlung zu molekularem Leitvermögen, 2. der optischen Tiefe τ_R längs des Halbmessers bei einer Photonen-Wellenzahl, die spektral aus exponentiell geschweiften Absorptionsbändern bestimmt wird, 3. einer turbulenten Reynolds–Zahl R_t. Es zeigt sich, daß die Strahlungs-Nusselt–Zahl linear zunimmt mit N_{rm} und mit τ_R bei kleinen Werten von τ_R, aber nahezu logarithmisch bei großen Werten von τ_R. Der Strahlungsaustausch nimmt auch zu mit größer werdender turbulenter Reynolds–Zahl, da die Turbulenz die Gasübertragbarkeit der effektiven Wandschicht verbessert.

ЛМОЛЕКУЯРНОЕ ГАЗОВОЕ ИЗЛУЧЕНИЕ И ЛАМИНАРНАЯ ИЛИ ТУРБУЛЕНТНАЯ ДИФФУЗИЯ ТЕПЛА В ЦИЛИНДРЕ С ВНУТРЕННИМ ИСТОЧНИКОМ ТЕПЛА

Аннотация — В работе рассматривается несерое излучение и диффузия тепла, происходяшие одновременно при термически и гидродинамически установившемся ламинарном или турбулентном течении в трубе с однородным внутренним источником тепла.

Основное интегро-дифференциальное уравнение тепловой энергии решается методом Галеркина для случая ламинарного течения и методами конечных разностей и численной итерации для турбулентного течения. Решения представлены для лучистого и конвективного чисел Нуссельта как функция отношения излучения к молекулярной проводимости N_{rm}, оптической глубины τ_R вдоль радиуса при фотонном волновом числе, спектрально расположенном в головной части экспоненциально затухающей полосы поглощения, и турбулентного числа Рейнольдса R_t. Найдено, что лучистое число Нуссельта увеличивается почти линейно с увеличением N_{rm} и линейно с увеличением τ_R при малых значениях τ, но примерно логарифмически при больших значениях τ_R. Величина лучистого переноса также растет с ростом турбулентности R_t, так как последняя улучшает эффективный коэффициент пропускания слоя газа на стенке.